ALPINE POLYPHASE METAMORPHISM IN METAPELITES FROM SIDIRONERO COMPLEX (RHODOPE DOMAIN, NE GREECE)

Mposkos, E.[1], Krohe, A.[2] and Baziotis, I.[1]

[1] National Technical University of Athens, School of Mining and Metallurgical Engineering, Division of Geological Sciences, 9, Polytechniou Str., Zografou (Athens),Greece, Phone ++3021-07722099

[2] Institute for Mineralogy, Laboratory of Geochronology University of Muenster Corrensstr.24, D-48149 Muenster, NRW, Phone: ++49-251-8333405, email: krohe@unimuenster.de

Abstract: Metamorphic mineral ages from garnet-kyanite gneisses in the area north of Xanthi documented a Jurassic and an Eocene metamorphic event in the Sidironero complex of the Rhodope domain. The two metamorphic events are well imprinted in the mineral assemblages, mineral compositions and textural relationships of metapelites within the Nestos Shear Zone in the Sidironero complex. The Jurassic event at HP-UHP metamorphic conditions is characterized by the mineral assemblage garnet-kyanite-Ti-rich phengite at the peak pressure. The Eocene metamorphic event at moderate HP conditions and minimum pressure > 0.9 GPa is characterized by the mineral assemblages St-Grt-Ms-Ky-Bt with garnet growth at the expense of kyanite or staurolite, and Grt-St-Ky-Bt with peak P-T conditions within the St+Bt+Ky stability field.

Keywords: metapelites, polyphase metamorphism, Rhodope, Sidironero Complex

1. Introduction

The Rhodope Domain occupies a central position in the Alpine belt, between the south west-verging Hellenides and the north-verging Balkanides. It mostly consists of medium-to high-grade pre-Alpine and Alpine metamorphic rocks and granitoids and represents the exhumed metamorphic core of the Alpine orogen of the Hellenides (Mposkos and Krohe, 2000; Ivanov et al., 2000).

Various authors have proposed several schemes for a subdivision of the Rhodope into different tectonic units (see Krohe and Mposkos, 2002 and references therein). Mposkos and Krohe (2000) and Krohe and Mposkos (2002) subdivided the Greek part of the Rhodope Domain into several superimposed tectonic complexes based on differing maximum P-T conditions, P-T paths, geochronological data (known so far), and including structural data constraining the kinematics of emplacement of different tectonic units. These units basically differ in evolution path of Alpine subduction and exhumation. The Vertiscos complex in the west part and the Kimi complex in the east part of the Rhodope Domain underwent mid-Mesozoic high pressure (HP)/ultra-high pressure (UHP) metamorphism and were exhumed to the upper crust in late Cretaceous to early Tertiary time. The underlying complexes Sidironero, Kardamos, Kechros and the lowermost Pangaeon complex including the Albite Gneiss Series underwent Tertiary HP metamorphism (early Eocene in the Sidironero complex, Liati and Gebauer, 1999) and were exhumed to the upper crust in late Eocene (Sidironero Complex) to Miocene time.

Since then, a huge number of new geochronological data have been published that bear witness to the imprint of at least two major Alpine metamorphic cycles, one in the mid-Mesozoic, the other in the mid-Cenozoic with an apparent gap of about 100 Ma in the Sidironero complex (Liati, 2005; Reischmann and Kostopoulos, 2002; Bosse et al., 2009). However, petrological evidences for both metamorphic events within single rocks are still lacking.

In this contribution we present petrological data from selected metapelites from the Sidironero complex, which combined with available geochronological data, indicate that the Sidironero complex underwent two Alpine prograde metamorphic events, a Jurassic HP/UHP metamorphism like that recorded in the overlying Kimi complex and an Eocene moderate HP one.

2. Geological Framework

The Sidironero complex consists of migmatitic quartz-feldspar–and pelitic gneisses, orthogneisses and marbles that host mafic and scarce ultramafic rocks. Partially amphibolitized kyanite eclogites and common eclogites indicate HP metamorphism at peak P-T conditions of >1.9 GPa and 700°C (Liati and Gebauer, 1999). Pelitic gneisses record granulite facies conditions by the mineral assemblage Grt-Ky-Bt-Pl-Kfs-Qtz-Rt (abbreviations after Martin, 1999) (Mposkos and Liati, 1993). Microdiamond inclusions in garnet from pelitic gneisses indicate that lithologies of the Sidironero complex underwent UHP metamorphism (Mposkos and Kostopoulos, 2001; Perraki et al., 2006).

Pre-Alpine ages for magmatic protoliths yielded SHRIMP U-Pb zircon dates (294±8 Ma) in orthogneisses (Liati and Gebauer, 1999). Alpine ages can be classified in two broad groups. The first group at ~185-140 Ma is represented by U-Pb SHRIMP ages in metamorphic rims on zircon, U-Th-Pb LA-ICPMS ages on monazite and Sm-Nd garnet-whole rock age from pelitic garnet-kyanite gneisses near Xanthi town (Liati, 2005; Bosse et al., 2006; Reischmann and Kostopoulos, 2002). This lithology has yielded evidence of diamond inclusions in garnet (Mposkos and Kostopoulos, 2001; Perraki et al., 2006). U-Pb SHRIMP zircon ages of 51 to 42 Ma from amphibolitized eclogites, ~ 36 Ma from cross-cutting pegmatites (Liati and Gebauer, 1999; Liati, 2005) and 55 to 39 Ma Th-Pb monazite ages from deformed pegmatites (Bosse et al., 2009) constrain the second group of the Alpine ages in the Sidironero complex.

A crustal scale shear zone several km in thickness (Nestos shear zone) separates the Sidironero complex and the underlying Pangaeon complex. This shear zone comprises lithologies of the UHP-HT Sidironero complex and the underlying HP Albite-Gneiss Series of Mposkos and Krohe (2000), which is a part of the Pangaeon complex (Mposkos et al., 1998). The Albite Gneiss Series consisting of orthogneisses, paragneisses with pre-mylonitic (pre-Alpine) migmatitic textures in outcrop scale, metapegmatites, minor amphibolites, metapelites and few marbles, record only the Tertiary Alpine metamorphism. In the Drama area, from south to north, the metamorphic grade of the Alpine metamorphism increases from the albite-epidote amphibolite facies to the middle amphibolite facies (Mposkos unpublished data). Pb-Pb evaporation and SHRIMP dating of zircons from orthogneisses

yielded Permo-Carboniferous ages (283-297 Ma) for their magmatic protoliths (Liati, 2005; Turpaud and Reischmann, 2010), and 38-40 Ma for the pegmatoid neosomes near the contact with the overlying Sidironero complex (Liati, 2005).

3. Evidence of polyphase metamorphism in metapelites

3.1. Petrography and Mineral Chemistry

Selected samples of metapelites from three localities of the Sidironero complex with textural relationships and mineral assemblages indicating polymetamorphic evolution are studied with optical microscopy, scanning electron microscopy and microprobe analysis. The sample localities are shown in figure 1.

Locality 1: (Fig. 1; coordinates N41^{0}16´59.6´´ E24^{0}24´45.3´´): In locality 1 garnet-kyanite gneisses with migmatitic textures show post-migmatitic mylonitisation. The mineral assemblage of the rock is: Grt+Ky+Bt+Ms+Qtz+Rt±Pl. Garnet porphyroblasts contain single grain inclusions of quartz, biotite, rutile, kyanite, zircon, xenotime, monazite, apatite and inclusions of composite grains consisting of Bt+Qtz+Rt±Xnt±Mnz (Fig. 2a) and Ky+Bt+Qtz±Ms. Rational crystal faces between composite inclusion and garnet host are common. Garnet shows corroded edges and is replaced by biotite and kyanite. The garnet has almost homogeneous composition ($Grs_5Prp_{22}Alm_{70}Sps_3$). Only the outermost rim shows diffusion zoning with decreasing MgO and increasing FeO, CaO and MnO contents (Table 1). Two generations of kyanite occur. Ky-1 occurs as single grain inclusions in garnet. Ky-2 is a major phase in the matrix. It commonly forms aggregates associated with biotite pseudomorphose after former Al-rich phase, probably garnet (Fig. 2b). Biotite inclusions in garnet show higher Mg# values compared to matrix biotite. The Mg# value in single grain biotite inclusions is 0.60, in biotite from polyphase inclusions consisting of Bt+Qtz+Rt± Xnt±Mnz 0.68 and in matrix biotite 0.44 (Table 2), reflecting biotite growth at different metamorphic conditions. Biotite from Bt+Ky+Ms+Qtz polyphase inclusions in garnet shows similar Mg# values to those of the matrix biotite.

Locality 2: (Fig. 1; coordinates N41^{0}20´21.9´´ E24^{0}12´33.1´´): Mylonitic garnet-kyanite gneisses 4 meters in thickness intercalated between underlying mylonitic and retrogressed amphibolites and marbles and overlaying quartz-feldspar gneisses. A
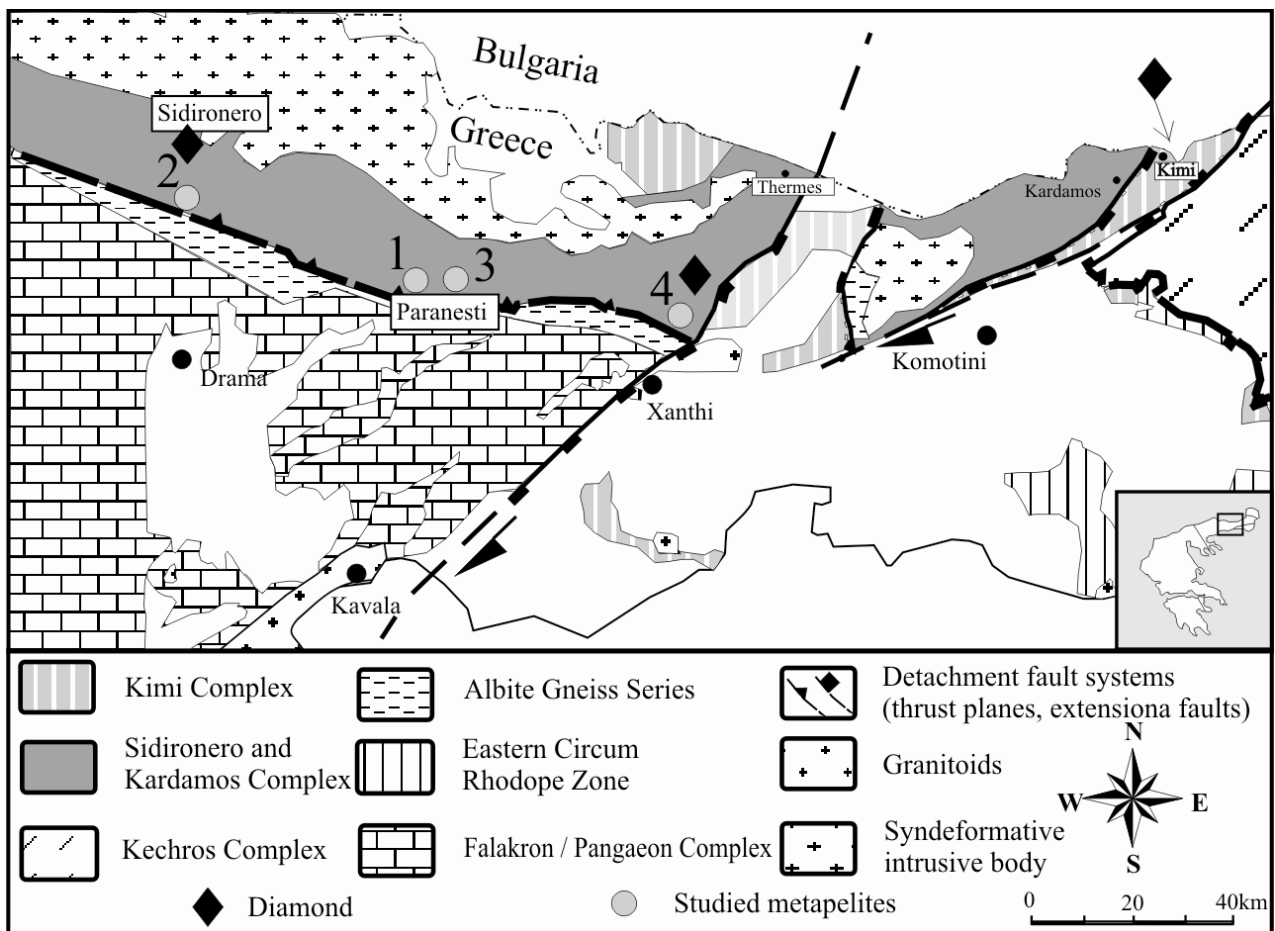
Fig. 1. Simplified geotectonic map of Central Greek Rhodope (after Mposkos and Krohe, 2000). Circles with numbers are localities of metapelites from Sidironero Complex, referred in the present work.

boudin of amphibolitized eclogite ~5m in length overlies the garnet-kyanite gneiss. The mineral assemblage of the garnet-kyanite gneisses is: Grt+Ky+Bt+Ms±St+Qtz±Pl+Rt±Ilm+Tur+Zr+Ap+Mnz.

Three generations of garnet are distinguished on textural and chemical criteria. Grt-1 (Grs_3 Prp_{18} Alm_{73} Sps_6) occurs as inclusion in kyanite porphyroblasts. Grt-2 (Grs_1 Prp_{26} Alm_{69} Sps_4) forms porphyroblasts up to 20 mm in size. It contains inclusions of rutile, quartz, muscovite, biotite, kyanite, staurolite, graphite, zircon and monazite. Exsolutions of rutile needles oriented in host garnet (triangular pattern, Fig. 2c) are common. Grt-3 (Grs_4 Prp_{18} Alm_{73} Sps_5) overgrows Grt-2 (Fig. 2d) and is commonly associated with matrix muscovite. It forms broad but irregular rims around parts of Grt-2 grains Grt-3 is rich in quartz and rutile inclusions. Inclusions of staurolite, muscovite and biotite are also present (Fig. 2d). Exsolutions of rutile needles are not present in Grt-3.

Two generations of kyanite and two of staurolite occur. Ky-1 forms porphyroblasts up to 15mm in size. Ky-1 contains inclusions of garnet (Grt-1), biotite, muscovite, rutile, quartz and rarely staurolite. Ky-2 (0.05-0.2 mm in size) is associated with matrix biotite, replaces Grt-2 and overgrows Ky-1. St-1 occurs as inclusions in Ky-1 and Grt-2. Matrix staurolite (St-2), if present, overgrows kyanite (Fig. 2e) and is associated with muscovite. It also occurs as inclusion in Grt-3 (Fig. 2d)

At least three generations of muscovite and two of biotite can be distinguished. Ms-1 and Bt-1 occur as inclusions in Ky-1 and Grt-2. Ms-2 is present as porphyroblasts up to 3 mm in size. It contains inclusions of garnet and kyanite, rutile needles interpreted as exsolutions (Fig. 2f), and flakes of biotite. Shape-preferred orientation of medium grained matrix muscovite (Ms-3) and biotite (Bt-2) define the main foliation of the rock. Matrix muscovite contains inclusions of kyanite grains with corroded edges. Rutile is the main Ti-ferous phase. It occurs as inclusions in Ky-1, Grt-1, Grt-2 and Grt-3 and in the rock matrix. Only matrix rutile is replaced by ilmenite.

Table 1. Representative garnet compositions of metapelites from the Sidironero complex.

	Locality-1		Locality-2				Locality-3					
	Grt-c	Grt-r	Grt-1c	Grt-2c	Grt-2r	Grt-3	Grt-1c	Grt-1r	Grt-2c	Grt-2r	Grt-1k	Grt-2k
SiO_2	37.97	37.45	37.65	38.11	37.17	37.52	37.56	37.00	36.90	36.90	37.70	36.79
Al_2O_3	21.43	21.14	21.18	21.54	20.93	21.06	21.15	20.89	20.81	20.80	21.25	20.80
FeO	31.84	32.02	32.91	31.50	33.48	31.70	33.42	35.10	23.98	31.13	32.94	33.95
MnO	1.53	3.49	2.54	1.78	2.79	4.67	2.34	3.70	13.06	5.19	1.64	4.43
MgO	5.56	3.62	4.45	6.64	3.50	3.62	4.87	2.70	1.08	3.24	5.52	2.28
CaO	1.67	2.11	1.07	0.22	1.73	1.33	0.45	0.62	4.12	2.01	0.71	1.40
Total	100.01	99.84	99.80	99.80	99.60	99.99	99.79	100.01	99.95	99.27	99.78	99.68
						12 oxygens						
Si	3.000	3.002	3.008	3.002	2.998	3.009	3.000	2.998	2.997	2.992	2.998	2.995
Al	1.996	1.998	1.994	2.000	1.990	1.992	1.991	1.994	1.992	1.988	1.992	1.996
Fe	2.105	2.147	2.199	2.076	2.258	2.127	2.233	2.378	1.629	2.111	2.190	2.311
Mn	0.102	0.237	0.172	0.119	0.190	0.318	0.160	0.254	0.898	0.356	0.111	0.306
Mg	0.655	0.432	0.530	0.779	0.421	0.433	0.580	0.326	0.130	0.391	0.654	0.277
Ca	0.142	0.182	0.092	0.019	0.149	0.115	0.039	0.054	0.359	0.175	0.061	0.122
Mg#	0.237	0.167	0.194	0.273	0.157	0.169	0.206	0.120	0.07	0.156	0.23	0.107

c=core, r=rim, s=inclusion in staurolite, k=inclusion in kyanite, Mg# = Mg/(Mg+Fe)

Locality 3 (Fig. 1; coordinates N41^{0}15´17.7´´ E24^{0}28´04.4´´): In locality 3 occur garnet-staurolite-kyanite schists with the mineral assemblage Grt+St+Ky+Bt+Ms±Chl±Sil±Pl+Rt+Ilm+Tur+Ap. Garnet is a major phase in the rock matrix. It also occurs as inclusions in staurolite and kyanite porphyroblasts (Fig. 2g). Two generations of garnet are distinguished based on chemical criteria (Table 1). Grt-1 (Grs$_2$ Prp$_{22}$ Alm$_{73}$ Sps$_3$ mean composition) shows diffusion zoning with decreasing the pyrope component from the core to the rim. Grt-2 has lower pyrope and higher spessartine component compared to Grt-1 and shows growth zoning with (Grs$_{12}$ Prp$_4$ Alm$_{55}$ Sps$_{30}$) core-and (Grs$_6$ Prp$_{13}$ Alm$_{69}$ Sps$_{12}$) rim compositions. Grt-2 contains inclusions of rutile, ilmenite and rarely chlorite and biotite. Staurolite and kyanite porphyroblasts (Ky-2) contain inclusions of garnet, biotite, muscovite, rutile and ilmenite (Fig. 2g). Grt-1 and Grt-2 are found as inclusions within a single kyanite porphyroblast (Fig. 2h). Kyanite also occurs as inclusions in staurolite (Ky-1; Fig. 2h). Chlorite is minor phase. Primary chlorite is observed as inclusion in Grt-2 and staurolite. Matrix chlorite is retrograde phase replacing biotite. Ilmenite is formed by replacing rutile. Ilmenite and rutile occur as inclusions in Grt-2, staurolite, kyanite and in the rock matrix. Fibrolitic sillimanite, if present, is always associated with matrix biotite. Replacement of kyanite by sillimanite is not observed.

3.2. Record of polymetamorphic evolution

Locality 1: The stable mineral assemblage Grt+Ky+Bt+Ms+Qtz indicates MP to HP metamorphism at upper amphibolite facies conditions (Fig. 3). The inclusions of kyanite and biotite in garnet porphyroblasts indicate garnet growth at the expense of kyanite+biotite according to the water conserving pressure dependent reaction:

$$2Ky+Bt+Qtz \rightarrow Grt+Ms \qquad (1)$$
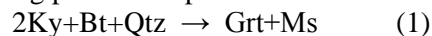
Pressures > 1.5 GPa and temperatures >650°C are obtained from reaction 1 (Fig. 3, curve 1). Inclusions of composite grains in garnet consisting of biotite+quartz+rutile±xenotime±monazite (Fig. 2a) suggest much higher P-T conditions. Such inclusions are common in garnets from the garnet-kyanite gneisses of the UHP Kimi complex and are interpreted to be formed from supercritical fluid or melt inclusions in garnet growing at UHP conditions (Mposkos and Krohe, 2006). Matrix biotite (Bt-2) and Ky-2 are formed during decompression according to reaction 1 (running from the right to the left), as indicated by the corroded edges of garnet, the decrease in Mg# at the rims of the garnet, and the lower Mg# values in matrix biotite compared to the Mg# values of single biotite grain inclusions in garnet (Table 2). The composite biotite+kyanite+quartz inclusions in garnet represent decomposition products of former phengite inclusions reacted with the host garnet during decompression.

Locality 2: Textural relationships and mineral compositions in the metapelites of locality 2 record two prograde metamorphic events. The first metamorphic event is recorded by the Ky-1, Grt-2, and Ms-2 porphyroblasts and their inclusions. The overprinting metamorphism is recorded by the matrix staurolite (St-2) overgrown by kyanite and Grt-3 overgrown by Grt-2 (Figs. 2d,e).
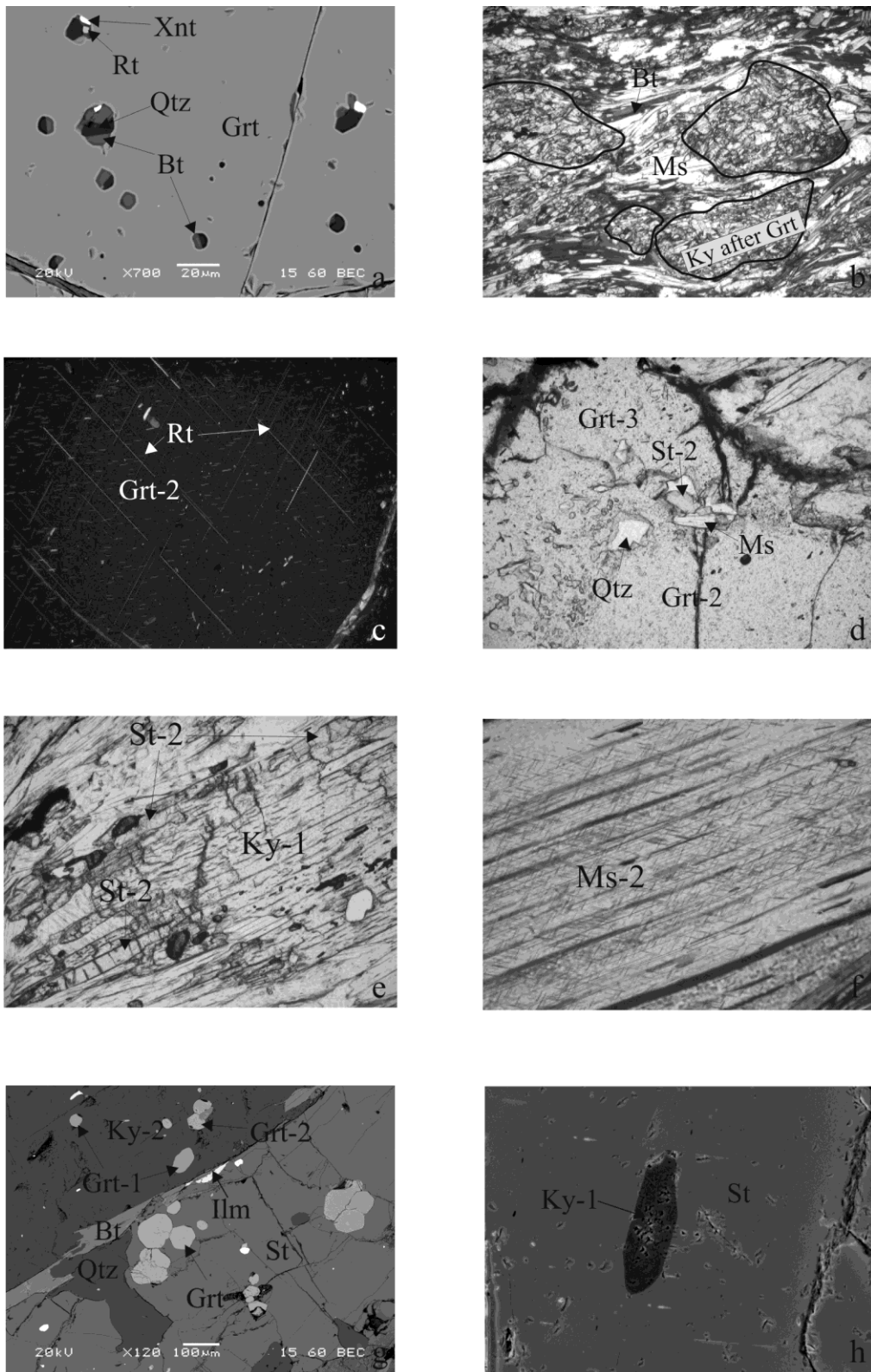
Fig. 2. Locality-1: (a) Composite inclusion consisting of Bt+Qtz+Rt in garnet porphyroblast. (b) Kyanite+biotite aggregates pseudomorphic after garnet. Locality-2: (c) Rutile needles exsolutions (triangular pattern) in garnet porhpyroblast (Grt-2); crossed pollars. (d) Part of garnet porphyroblast (Grt-2) overgrown by new garnet (Grt-3). Grt-3 contains quartz, staurolite (St-2), muscovite (Ms) and biotite (Bt) inclusions. (e) Matrix staurolite (St-2) overgrows kyanite porphyroblast (Ky-1). (f) Muscovite porphyroblast (Ms-2) with rutile needle exsolutions. Locality-3: (g) Staurolite and kyanite (Ky-2) porphyroblasts with inclusions of garnet (Grt-1 and Grt-2). (h) Kyanite (Ky-1) inclusion in staurolite. (a), (g), (h): SEM images and (b),(c), (d), (e), (f): microphotographs.

The inclusions of Grt-1, St-1, Bt and Ms in Ky-1 porphyroblasts indicate formation of kyanite in a prograde path of metamorphism according to the reaction:

$$St-Ms \rightarrow Grt+Ky+Bt+H_2O \qquad (2)$$

Inclusions of kyanite with corroded edges in Grt-2 porphyroblasts indicate garnet growth at the ex-pense of kyanite (+biotite) according to reaction 1 with pressure increase. Pressures > 1.5 GPa are obtained from reaction 1 (Fig. 3, curve 2). The presence of microdiamond inclusions in garnet porphyroblasts from metapelites of locality 2 (Schmidt et al., 2010), constrains the minimum pressure at 3.5 GPa for assumed temperature of 800°C. We consider that at peak P-T conditions the temperature
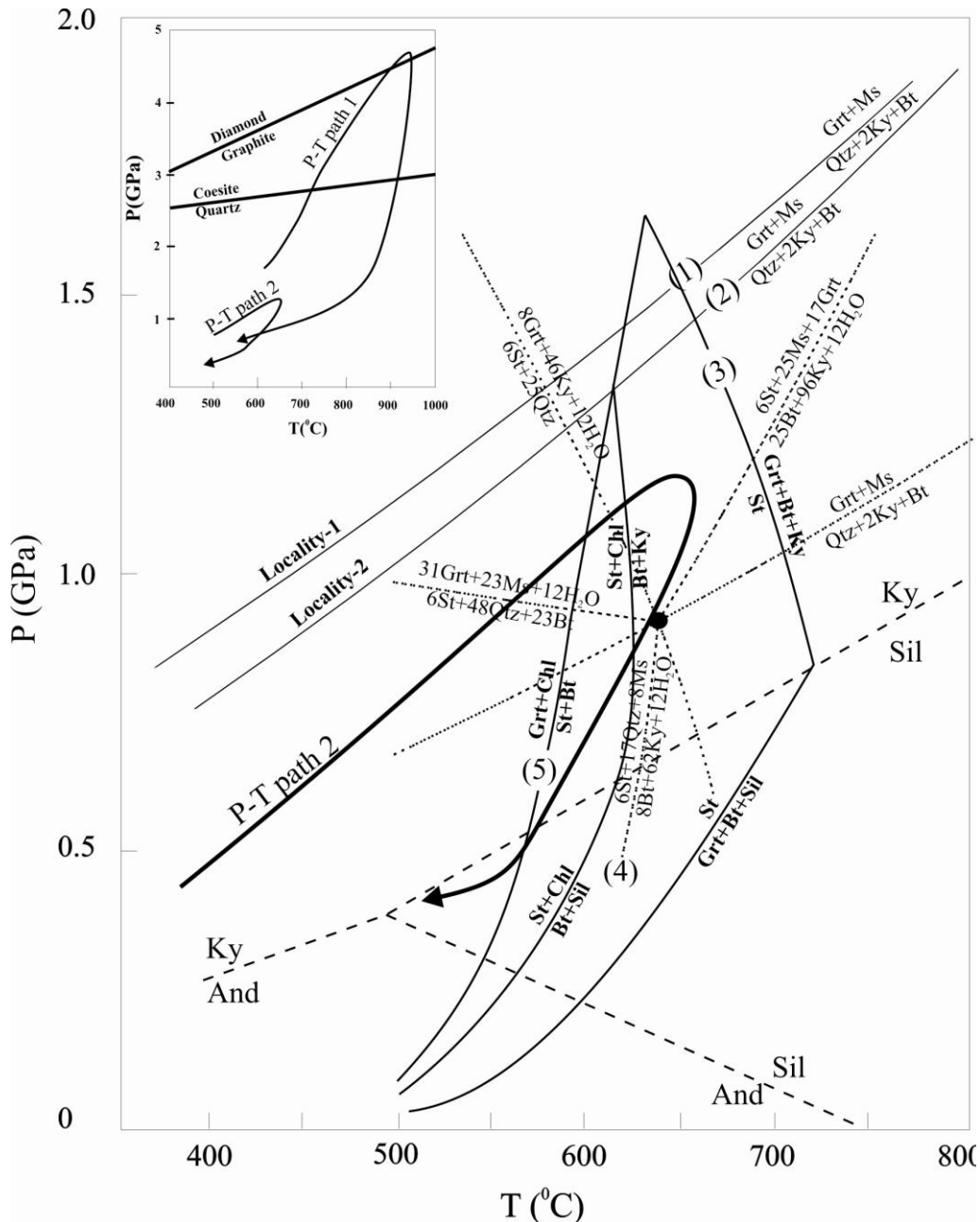

Fig. 3. P-T diagram showing univariant reaction curves in the system KFMASH (taken from Spear 1995). Dotted reaction curves are calculated with the TWEEQU software for the system St+Grt+Ky+Bt+Ms+Qtz+H₂O using mineral compositions representing the second prograde metamorphic event in locality-2. Reaction curves 1 and 2 are calculated using garnet core - biotite inclusion compositions from garnet porphyroblasts of localities 1 and 2. Insert: The Jurassic UHP metamorphism is shown in P-T path 1 and the Eocene intermediate HP metamorphism in P-T path 2.

was very high as shown by the rutile needle exsolutions in garnet and muscovite porphyroblasts (Figs. 2c,f), which suggest that the UHP assemblage contained Ti-rich garnet and Ti-rich phengite. High-Ti phengites are reported from UHP-HT gneisses from Kokchetav massif in Kazakhstan (Hermann et al., 2001) and Ti-rich garnets in eclogites from Sulu UHP terrane and from UHP-HT experiments (Zhang et al., 2003). Matrix biotite (Bt-2) and matrix kyanite (Ky-2) are formed during decompression according to reaction 1 (running from the right to the left), as indicated by the corroded edges of garnet porphyroblasts, the decrease in Mg# at the rims of the garnet, and the lower Mg# values in the matrix biotite compared to the Mg# values of biotite inclusions in garnet (Table 2). Matrix staurolite (St-2) overgrew kyanite (Fig. 2e), indicating that it has been formed by consuming kyanite according to reaction 4 in figure 3. For staurolite formation, the intrusion of water in the rock is needed. Calculated reaction curves for the system $St+Grt+Ky+Bt+Ms+Qtz+H_2O$ using real mineral compositions (Tables 1 and 2) show that staurolite coexists with garnet (Grt-3) at pressures higher than the invariant point (> 0.9 GPa) (Fig. 3). The absence of rutile exsolutions in Grt-3 indicates that Grt-3 grew at much lower temperatures and pressures than Grt-2. Syndeformational ilmenite formed during decompression replaced matrix rutile. Applying the GRAIL geobarometer yields pressures of 0.5 GPa indicating that the dominant foliation in the metapelite formed during the exhumation.

Locality 3: The second prograde metamorphic event is well recorded in the metapelites from locality 3. Grt-1, Rt and Ky-1 are relics of a former metamorphic event at higher P-T conditions as indicated by a) the higher pyrope component in Grt-1 (22%) compared to that of Grt-2 (4-13%), b) the different patterns of chemical zoning (diffusion zoning in Grt-1, growth zoning in Grt-2), c) the kyanite inclusions (Ky-1) in staurolite, d) the rutile inclusions in Grt-1 and e) the replacement of rutile by ilmenite. The presence of ilmenite replacing rutile in the matrix and as inclusion in garnet (Grt-2), staurolite and kyanite indicates that the second prograde metamorphism started within the ilmenite stability field. The first stage of metamorphism was within the garnet+chlorite+biotite stability field as indicated by the chlorite and biotite inclusions in Grt-2. Staurolite+biotite were formed at the expense of garnet and chlorite (Fig. 3, curve 5). With further increase in P-T conditions kyanite+ biotite was formed consuming staurolite and chlorite. Fibrolitic sillimanite associated with biotite was formed during decompression as the P-T path crosses the kyanite-sillimanite boundary.

Table 2. Representative composition of biotite, muscovite and staurolite from metapelites of the Sidironero complex.

	Locality-1			Locality-2						Locality-3		
	Bt-1g	Bt-2g	Bt-3m	Bt-g2	Bt-k	Bt-m	Ms-p	St-g2	St-m	St	Bt-st	Bt-m
SiO_2	38.54	37.95	36.54	37.50	36.02	35.92	47.41	28.26	28.10	28.30	35.77	35.52
TiO_2	2.57	3.11	1.83	1.38	1.39	1.77	1.21	0.83	-	-	1.32	1.85
Al_2O_3	17.45	17.47	18.14	20.53	19.47	19.24	32.51	52.70	53.03	53.85	19.33	19.22
FeO	14.22	11.86	19.51	11.05	15.41	16.72	1.10	10.09	12.67	13.78	19.89	20.31
MnO	-	-	-	-	-	-	-	0.12	0.46	-	-	-
MgO	11.85	14.16	8.59	14.88	12.60	11.20	1.15	2.64	1.62	1.76	9.12	8.42
ZnO	-	-	-	-	-	-	-	3.17	2.45	0.43	-	-
NaO	-	-	-	-	-	-	-	-	-	-	-	-
K_2O	10.39	10.34	9.98	10.38	9.99	9.83	11.48	-	-	-	9.58	9.55
Total	95.01	94.89	94.58	95.72	94.80	94.69	94.86	97.75	98.33	98.12	95.01	94.86
	22 oxygens							47 oxygens		22 oxygens		
Si	5.730	5.600	5.606	5.449	5.407	5.432	6.356	8.002	7.996	7.999	5.463	5.448
Ti	0.287	0.345	0.211	0.151	0.157	0.201	0.122	0.177	-	-	0.152	0.213
Al	3.057	3.039	3.280	3.514	3.445	3.430	5.138	17.63	17.79	17.94	3.479	3.475
Fe	1.768	1.464	2.504	1.343	1.934	2.115	0.123	2.394	3.015	3.257	2.541	2.605
Mn	-	-	-	-	-	-	-	0.029	0.111	-	-	-
Mg	2.625	3.113	1.965	3.222	2.819	2.525	0.229	1.117	0.687	0.743	2.076	1.925
Zn	-	-	-	-	-	-	-	0.664	0.515	0.090	-	-
Na	-	-	-	-	-	-	-	-	-	-	-	-
K	1.971	1.946	1.953	1.924	1.897	1.897	1.963	-	-	-	1.866	1.868
Mg#	0.60	0.68	0.44	0.70	0.59	0.54	0.65	0.32	0.18	0.19	0.45	0.42

g2, k, st = inclusion in Grt-2, Kyanite and staurolite respectively, m=matrix, p=porphyroblast

4. Discussion and Conclusions

The mineral assemblages and textures of the metapelites from locality 2 indicate that the metapelites underwent two distinct metamorphic events; the first at HP or UHP (documented by the microdiamond inclusions in garnet Schmidt et al. 2010) and the second at moderate HP.

North of Xanthi (locality 4 in figure 1), the garnet-kyanite gneisses containing dispersed amphibolitized eclogite boudins, have the mineral assemblage Grt-Ky-Ms-Bt-Pl-Qtz±Kfs±St±Sil+Rt+Ilm. Textures and mineral compositions are similar to those described in locality 2 (Mposkos and Liati 1993). Microdiamond inclusions in garnet porphyroblasts are described by Mposkos and Kostopoulos (2001) and Perraki et al. (2006). Two major Alpine metamorphic events are documented by dating metamorphic minerals from the garnet-kyanite gneisses of the locality 4; a Jurassic and an Eocene (Liati, 2005; Bosse et al., 2009 and references therein). Although mineral ages from the studied metapelites of the three localities are not available, we consider that the HP-UHP event documented in localities 1 and 2 as well as the Grt-1, Ky-1 and Rt relicts from locality 3 are Jurassic in age and the moderate HP overprinting event documented in localities 2 and 3 occurred in Eocene.

Jurassic ages are also reported from the diamond-bearing garnet-kyanite gneisses from the Kimi complex in the Eastern Rhodope (Bauer et al. 2007). The Kimi complex tectonically overlies the Sidironero complex (Mposkos and Krohe, 2000; Krohe and Mposkos, 2002). The metapelites from both complexes seems to have a common Jurassic tectonometamorphic evolution (Mposkos and Liati, 1993; Liati, 2005; Bauer et al., 2007). We hence interpret the Sidironero and Kimi complexes to represent a single, originally connected tectonic block of pre-Alpine continental crust involved in the Jurassic subduction of a branch of the northward subducted Vardar-Axios Ocean under the European continent. The final tectonic juxtaposition of both complexes against each other occurred by Tertiary tectonic processes.

In the Kimi and Sidironero complexes the orthogneisses (most of them are migmatites) yielded U-Pb and Pb-Pb zircon ages in the range of ~165 to 135 Ma, which are interpreted as dating the magmatic protoliths from magmas produced in a magmatic arc setting (Turpaud and Reischmann, 2010; Cornelius, 2008). The wide (20 to 60 Ma) range of U-Pb zircon ages within a single hand specimen, the presence of many pre-Alpine (mostly Variscan) inherited zircon cores in the samples dated by SHRIMP, and that most of the dated gneisses are migmatites (the orthogneiss near the Sidiro village in east Rhodope contains boudins of partially amphibolitized eclogites), suggest that the late Jurassic-early Cretaceous ages of the orthogneisses probably record successive stages of the metamorphic evolution (including high degree of melting) of pre-Alpine magmatic protoliths in a thickened crust after the HP/UHP metamorphic event.

The Nestos shear zone, that contains the studied metapelites, can be traced for about 80 km from Xanthi to the west, to the Bulgarian border. The shear zone includes lithologies from the overlying Sidironero complex, that records two Alpine prograde metamorphic events, one in Jurassic and a second in Eocene (Liati, 2005; Bosse et al., 2009 and references therein), and the underlying Albite-Gneiss-Series that record only one Alpine metamorphic event in the Eocene (Liati, 2005). We consider the migmatitic orthogneiss, which occurs near and below of the metapelites from locality-2 as the upper part of the Albite-Gneiss-Series. At this locality the metamorphic conditions reached those of the granite wet-melting. The U-Pb zircon ages of Liati (2005) only record pre-Alpine and Eocene events, but not any Jurassic event. Both complexes are thrust over the marbles of the Pangaeon complex. Two of the presently known four UHP metamorphic localities in the Greek Rhodope Mountains occur along the Nestos shear zone of the Sidironero complex and two of them within the overlying Kimi complex. The Nestos shear zone represents a major SW directed thrust occurred in Eocene in a compressional regime by underthrusting of the Pangaeon complex (including the Albite-Gneiss Series) under the southern borders of the European continent, part of which was the Kimi complex. With a tectonic erosion mechanism slices of the Kimi complex are brought in the underthrusting plate and suffered the Eocene prograde moderate HP metamorphism, with a P-T path correspond to geothermal gradient $< 17^{\circ}$C/km.

References

Bauer, C., Rubatto, D., Krenn, K., Proyer, A. and Hoinkes, G., 2007. A zircon study from the Rhodope Metamorphic Complex, N-Greece. Time recorded of a multistage evolution. Lithos, 29, 207-228.

Bosse, V., Boulvais, P., Gautier, P., Tiepolo, M., Ruffet, G., Devilal, J.L. and Cherneva, Z., 2009. Fluid-induced disturbance of the monazite Th-Pb chronometer: In situ dating and element mapping in pegmatites from the Rhodope (Greece, Bulgaria). Chemical Geology 261, 286-302.

Cornelius, N.-K., 2008. UHP metamorphic rocks of the Eastern Rhodope Massif, NE Greece: new constraints from petrology, geochemistry and zircon ages. Ph.D.Thesis University of Mainz.

Hermann, J., Rubatto, D., Korsakov, A., and Shatsky, V.S., 2001. Multiple zircon growth during fast exhumation of diamondiferous, deeply subducted continental crust (Kokchetav Massif, Kazakhstan). Contributions to Mineralogy and Petrology, 141: 66-82.

Ivanov, Z., Kolkovski, B., Dimov, D., Sarov, S. and Dobrev, S., 2000. Structure, Alpine evolution and metallogeny of the Central Rhodopes area, South Bulgaria. Abstract Volume, ABCD-GEODE, Borovets, 30.

Krohe, A. and Mposkos, E., 2002. Multiple generations of extensional detachments in the Rhodope Mountains (N.Greece): evidence of episodic exhumation of high-P rocks. In: Blundell, D.J., Neubauer, G. and Von Quant, A. (eds.): The timing and location of major ore deposits in an evolving orogen. Geological Society of London, Special Publication, 204, 151-178.

Liati, A., and Gebauer, D., 1999. Constraining the prograde and retrograde P-T-t path of Eocene HP rocks by SHRIMP dating of different zircon domains: inferred rates of heating, burial, cooling and exhumation for central Rhodope, northern Greece. Contributions to Mineralogy and Petrology,, 135, 340-354.

Liati, A., 2005. Identification of repeated Alpine (ultra) high-pressure metamorphic events by U-Pb SHRIMP geochronology and REE geochemistry of zircon: the Rhodope zone of Northern Greece. Contributions to Mineralogy and Petrology, 150, 608-630.

Martin, R.F., 1998. Symbols of the rock-forming minerals. The Nomenclature of minerals: A compilation of IMA reports. International Mineralogical Association 98 Toronto, 148-149.

Mposkos, E., and Liati, A., 1993. Metamorphic evolution of metapelites in the high-pressure terrane of the Rhodope zone, Northern Greece. Canadian Mineralogist, 31: 401-424.

Mposkos, E., Chatzipanagis, I., and Papadopoulos, P., 1998. New data on the boundaring the Pangaeon and Sidironero tectonic units in Western Rhodope. Bulletin of the Geological Society of Greece, 32/1, 13-21. (In Greek with English abstract)

Mposkos, E., and Krohe, A., 2000. Petrological and structural evolution of continental high pressure (HP) metamorphic rocks in the Alpine Rhodope Domain (N.Greece). In: Proceedings of the 3rd International Conference on the Geology of the Eastern Mediterranean, Nicosia, Cyprus, 1999. Edited by I.Panayides, C.Xenophontos, and J. Malpas. Geological Survey, Nocosia, Cyprus, pp. 221-232.

Mposkos, E., and Kostopoulos, D., 2001. Diamond, former coesite and supersilicic garnet in metasedimentary rocks from the Greek Rhodope: a new ultrahigh-pressure metamorphic province established. Earth and Planetary Science Letters, 192, 497-506.

Mposkos, E., and Krohe, A., 2006. Pressure-temperature-deformation paths of closely associated ultra-high pressure (diamond-bearing) crustal and mantle rocks of the Kimi complex: implications for the tectonic history of the Rhodope Mountains, northern Greece. Canadian Journal of Earth Sciences, 43, 1755-1776.

Perraki, N., Proyer, A., Mposkos, E., Kaindl, R., and Honkes, G., 2006. Raman micro-spectroscopy on diamond, graphite and other carbon polymorphs from the ultrahigh-pressure metamorphic Kimi Complex of the Rhodope Metamorphic Province, NE Greece. Earth and Planetary Science Letters, 241, 672-685.

Reischmann, T. and Kostopoulos, D., 2002. Timing of UHPM in metasediments from the Rhodope Massif, N.Greece. Proceedings Goldschmidt Conf., Davos, Switzerland, p. 634.

Schmidt, S., Nagel, T. and Froitzheim, N., 2010. A new occurrence of micro-diamond-bearing metamorphic rock, SW Rhodope, Greece. European Journal of Mineralogy, 22/2, 189-198.

Spear, F., 1995. Metamorphic Phase Equilibria and Pressure-Temperature-Time Paths. Mineralogical Society of America, Monograph, p. 799.

Turpaud, P., and Reischmann, T., 2010. Characterization of igneous terranes by zircon dating: implications for UHP occurrences and suture identification in the Central Rhodope, northern Greece. International Journal of Earth Sciences, 99, 567-591.

Zhang, R.Y., Zhai, S.M., Fei, Y.W. and Liou, Z.G., 2003. Titanium solubility in coexisting garnet and clinopyroxene at very high pressure: The significance of exsolved rutile in garnet. Earth and Planetary Science Letters, 216, 591-601.